Figs. 2–4 is shown in detail in Fig. 11 where we plot $(\Delta\alpha/c_0)$ (uncorrected) and $(\Delta\alpha/c_0)$ (corrected by ϕ) as a function of $y_0^{\pm}$. The step-junction absorption curve is the same as the theoretical absorption curve of Fig. 4, except for the ordinate scale factor. The -0.45 curve is calculated from Eq. (1) using ϕ obtained from Eq. (A2) for $\mathcal{E}$ having the dependence

$$\mathcal{E}(x)=\mathcal{E}_m[1-(x/x_0)^{1.22}].$$

We note that there is very little difference between the step junction and the -0.45 junction curves. They may be brought into coincidence below the bandgap, where the effective mass is determined, by a shift of 0.018 in $y_0^{\pm}$, (equivalent to decreasing the bandgap by 0.13 meV) and a change of scale of $y_0^{\pm}$ by a factor of 0.04 (equivalent to multiplying the reduced mass by a factor of 0.885). This correction results in a negligible shift of the band edge since the spectral resolution was approximately four times greater, and changes the experimentally determined reduced mass to $0.16m_0$. Above the edge, the effect of ϕ is negligible. The correction does not affect the qualitative behavior of the data, and affects the quantitative behavior by only a few percent. The effect on the $C\propto V^{-0.413}$ germanium junction used for the indirect-transition measurements shown in Figs. 5 and 6 is comparable and is neglected.

We have also evaluated Eq. (A2) for the -0.45 germanium junction used for the direct-transition measurements of Figs. 7–10. The theoretical curves of Figs. 9 and 10, calculated from Eq. (5) for a step junction, can shift as much as 20% at about 30 meV below threshold, but remain essentially unchanged above. However, there is almost no effect on the value of the experimentally determined reduced mass, as the 20% shift is reached about -30 meV below threshold in Fig. 10 and remains constant for lower energies. We, therefore, neglect the ϕ correction for these measurements and the ordinates of all figures are given as approximately equal to $\Delta\alpha$.

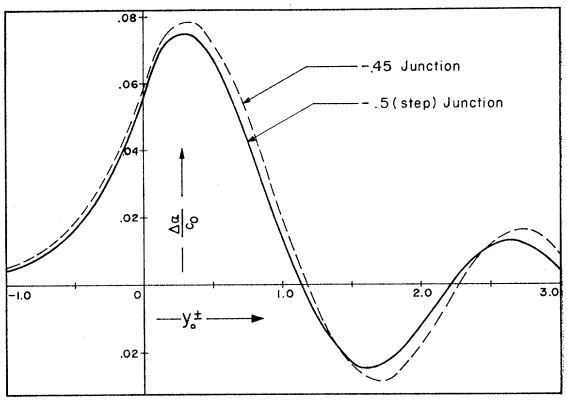

FIG. 11. $\Delta\alpha/c_0=[\alpha(\omega,\mathcal{E})-\alpha(\omega,0)]c_0^{-1}$ for a step junction and a junction with $C\propto V^{-0.45}$ for phonon-assisted transitions. The step-junction curve is the integral of Eq. (3) for an Airy-function normalization of $\pi^{-1/2}$ (the normalizations of Refs. 13 and 14).

Since exciton effects have not been included, we are unable to make a correction for this effect, and this may introduce larger errors in the ϕ correction.

PHYSICAL REVIEW VOLUME 145, NUMBER 2 13 MAY 1966

Solvable Model of a Hydrogenic System in a Strong Electric Field: Application to Optical Absorption in Semiconductors

C. B. DUKE AND M. E. ALFERIEFF*
General Electric Research and Development Center, Schenectady, New York
(Received 22 November 1965)

A model potential is proposed which, in parabolic coordinates, consists of the Coulomb potential near the origin and linear terms in the electric-field potential far from the origin. The eigenfunctions of the model potential are obtained exactly and analytically. An expression for the optical-absorption coefficient for excitons in an electric field is derived. Selection rules for allowed and forbidden vertical transitions are obtained. Numerical calculations of the line shapes of the lowest three exciton peaks are shown to be in agreement with existing experimental data. The model predicts no asymptotic alteration of the low-frequency Franz-Keldysh edge by the Coulomb interaction and a shift to lower energies of the continuum absorption near the zero-field band gap. Comparison of the predictions of the model with those of perturbation theory in the region of the low-field exciton peaks indicates that the model does not correctly yield the positions of the peaks but does qualitatively describe their broadening and eventual disappearance in an increasing electric field. Experiments measuring the quenching field for exciton peaks in the alkali halides and rare-gas solids are proposed as a method of ascertaining the spatial extent of the associated excitons.

I. INTRODUCTION

DISCUSSION of the spectra of a hydrogen atom in an external electric field dates from the pre-quantum-theory applications of the Bohr model to successfully interpret the Stark effect in atomic hydrogen.[1] The applications of quantum theory to the de-

* Present address: Department of Applied Mathematics, Massachusetts Institute of Technology, Cambridge, Massachusetts.

[1] The original papers on the Stark effect are summarized in, e.g., (a) E. U. Condon and G. H. Shortley, *The Theory of Atomic Spectra* (Cambridge University Press, Cambridge, England, 1963), Chap. 17; (b) H. E. White, *Introduction to Atomic Spectra* (McGraw-Hill Book Company, Inc., New York, 1934), Chap. 20.

scription of these spectra fall into two categories. The perturbation-theory calculation of the (Stark) shift of the hydrogenic energy levels was pioneered by Schrödinger and Epstein.[1,2] The calculation of the broadening of those levels by the electron tunneling to the free-field region outside the nuclear potential was first discussed by Oppenheimer,[3] who developed a variant of first order perturbation theory to study this effect. These calculations were considerably extended by Lanczos[4] who also presented a "derivation" of the WKBJ tunneling probability utilized in the theory of alpha decay[5] and more recently in the description of electron tunneling between thin films.[6]

The existence of relatively sharp energy levels in a combined Coulomb potential and external electric field is well known to be a consequence of the fact that, despite the continuous nature of the energy spectrum, the character of the wave function can change drastically within small energy intervals. The work described above is confined to a description of the narrow energy region near the Coulombic levels in the absence of the field. It is based on the assumption that the electron has little probability of tunneling out of its Coulombic potential well. However, optical-absorption experiments in solids deal with sufficiently strong electric fields that the hydrogenic electron-hole system has an appreciable probability of being ionized by the field. (In the direct edge of Ge, auto-ionization of the lowest hydrogenic state occurs at fields $F\sim1000$ V/cm.) Furthermore, recent experiments using phase sensitive detection of the electric-field-modulated absorption[7,8] and reflectivity[9] of semiconductors require for their analysis a calculation of the absorption coefficient at energies far below the lowest hydrogenic energy eigenvalue. Although many authors[10] have calculated the absorption in the absence of the Coulomb attraction between the electron and hole, the analysis given herein is the first to include the influence of this attraction.[11]

In order to provide an adequate interpretation of the optical absorption experiments, we must extend the original Stark-effect calculations to include both a description of strong electric fields and an evaluation of the absorption not only in the vicinity of the energies of the Stark levels, but also between and below these energies. We achieve these extensions of the theory by shifting our attention to the calculation of wave functions rather than approximate eigenvalues with their tunneling-induced widths. This change in emphasis is accomplished by following the theory of absorption due to Elliot[12] who demonstrated that the absorption coefficient is simply related to the effective-mass envelope function (wave function) and its derivatives evaluated at the origin. In order to calculate the wave functions in terms of known functions, we propose a model of a hydrogenic system in a strong electric field which consists of the Coulomb potential alone near the origin and the linear electric field far from the origin. The wave functions associated with the model potential are evaluated analytically (treating the energy as a continuously varying parameter). Therefore, we achieve an exactly solvable model giving resonant line shapes in the absorption coefficient but not limited to energy regions close to the resonance lines or to moment expansions. Our model calculation constitutes, to the best of the authors' knowledge, the first exact solution to the Schrödinger equation for a potential, other than the rectangular barrier,[13] exhibiting quasi-stationary states in the continuum. The triangular barrier problem has been treated exactly[14] but with emphasis on the calculation of the transmission coefficient and not on the existence of the quasi-stationary states which result if the eigenvalue spectrum is made nondegenerate by the imposition of an infinite potential on one side of the barrier.

In Sec. II we specify the model potential. In Sec. III the eigenfunctions associated with it are obtained. The derivation of the optical-absorption boundary value problem is given in Sec. IV together with a presentation of numerical calculations of the absorption coefficient and a discussion of relevant experiments. In the final section, we present a critique of the model, a proposal of some experiments, and a synopsis of our conclusions concerning optical absorption.

II. DEFINITION OF THE MODEL

The Schrödinger equation for a stationary hydrogenic system in an external electric field, F, is given by[15]

$$(\tfrac{1}{2}\Delta-\mathcal{E}z+r^{-1}+E)\phi_E(\mathbf{r})=0, \tag{2.1a}$$

$$\mathcal{E}=\frac{|e|\mu a_B{}^3F}{\hbar^2}=1.94\times10^{-10}\left(\frac{m}{\mu}\right)^2\epsilon_0{}^3F(\mathrm{V/cm}), \tag{2.1b}$$

[2] E. Schrödinger, Ann. Physik **80**, 457 (1926); P. S. Epstein, Phys. Rev. **28**, 695 (1926).
[3] J. R. Oppenheimer, Phys. Rev. **31**, 66 (1928).
[4] C. Lanczos, Z. Physik **62**, 28 (1930); **65**, 518 (1930); **68**, 204 (1931).
[5] See, e.g., R. W. Gurney and E. U. Condon, Phys. Rev. **33**, 127 (1929) and G. Gamow, Z. Physik **51**, 204 (1928).
[6] J. Bardeen, Phys. Rev. Letters **6**, 57 (1961); W. A. Harrison, Phys. Rev. **123**, 85 (1961).
[7] See, e.g., M. Chester and P. H. Wendland, Phys. Rev. Letters **13**, 193 (1964); A. Frova and P. Handler, Phys. Rev. **137**, A1857 (1965). More extensive references can be found in these articles.
[8] P. H. Wendland and Marvin Chester, Phys. Rev. **140**, A1384 (1965).
[9] B. O. Seraphin and R. B. Hess, Phys. Rev. Letters **14**, 138 (1965); B. O. Seraphin and N. Bottka, *ibid.* **15**, 104 (1965).
[10] Although W. Franz [Z. Naturforsch. **13a**, 484 (1958)] and L. V. Keldysh, Zh. Eksperim. i Teor. Fiz. **34**, 1138 (1958) [English transl.: Soviet Phys.—JETP **7**, 788 (1958)] gave the original calculations of the absorption coefficient, our treatment is most similar to that of K. Tharmalingam, Phys. Rev. **130**, 2204 (1963).
[11] F. Seitz [Phys. Rev. **76**, 1376 (1949)] has given estimates of the exciton auto-ionization fields but did not attempt to calculate the optical absorption coefficient. An abbreviated version of the analysis described has been presented by C. B. Duke, Phys. Rev. Letters **15**, 625 (1965).
[12] R. J. Elliot, Phys. Rev. **108**, 1384 (1957).
[13] See, e.g., Enrico Fermi, *Nuclear Physics* (University of Chicago Press, Chicago, Illinois, 1950), p. 61.
[14] R. H. Fowler and L. Nordheim, Proc. Roy. Soc. (London) **A119**, 173 (1928).
[15] L. D. Landau and E. M. Lifschitz, *Quantum Mechanics* (Addison-Wesley Publishing Company, Inc., Reading, Massachusetts, 1958), p. 251.

in which μ is the reduced mass of the hydrogenic system; a_B is the Bohr radius, e is the charge on an electron, m is the mass of an electron, and ϵ_0 is the (static) dielectric constant of the medium in which the system is contained. Length is measured in units of a_B and energy in units of $E_0=\hbar^2/\mu a_B^2$. Equation (2.1a) has a continuous spectrum of both positive and negative eigenvalues, E. We confine our attention to the negative eigenvalues and define a new variable, n, by

$$n\equiv 1/(-2E)^{1/2}, \quad E=-1/2n^2, \tag{2.2}$$

so that in the $\mathcal{E}\to 0$ limit, the eigenvalue spectrum becomes discrete with the integral values of n giving the allowed values of E.[15]

It is well known[2,15] that Eq. (2.1a) is separable in parabolic coordinates:

$$x=(\xi\eta)^{1/2}\cos\phi, \quad y=(\xi\eta)^{1/2}\sin\phi, \quad z=\tfrac{1}{2}(\xi-\eta). \tag{2.3}$$

We find

$$\phi_E(\mathbf{r})=(2/\pi)^{1/2}\chi_1(\rho_1)\chi_2(\rho_2)e^{im\phi}/(n^2\rho_1\rho_2)^{1/2}, \tag{2.4a}$$

$$\rho_1=\xi/n, \quad \rho_2=\eta/n; \tag{2.4b}$$

$$d^2\chi_i/d\rho_i^2+[-\tfrac{1}{4}-U_i(\rho_i)]\chi_i=0, \tag{2.4c}$$

$$U_i(\rho_i)=(m^2-1)/\rho_i^2-(n_i+\tfrac{1}{2}(1+|m|))/\rho_i -(-1)^i\mathcal{E}n^3\rho_i/4, \tag{2.4d}$$

$$n_1+n_2=n-1-|m|. \tag{2.4e}$$

Equations (2.4c) lead to a four-term recursion relation so that their solution cannot be expressed in terms of tabulated functions. The boundary condition that χ_1 be normalizable renders numerical integration of the equation impractical. If $|m|\leq 1$, the singularity of the potentials $U_i(\rho_i)$ at the origin renders the WKBJ approximation invalid there. We propose as a lowest order approximation to the solution of Eqs. (2) those obtained from a model potential which is a Coulombic potential inside a cutoff value $\rho_i^{(0)}$ and a linear electric-field potential outside $\rho_i^{(0)}$.

Corrections to the model may be calculated by treating the difference between Eqs. (2.4d) and the model potential as a perturbation. Minimizing the first order corrections to the energy would provide a rational basis for selecting the cutoff $\rho_i^{(0)}$. Such a selection procedure is numerically complicated because of its self-consistent nature. It also yields different values of $\rho_i^{(0)}$ for each quantum state. In this paper we use a cutoff which is independent of the quantum state. We select the $\rho_1^{(0)}$ and $\rho_2^{(0)}$ values to be equal and specified by

$$\rho_1^{(0)}=\rho_2^{(0)}=x_0/n. \tag{2.5a}$$

In our calculations of optical absorption in direct band-gap semiconductors, we require only the $|m|=0$ solutions to Eqs. (2.4). We are primarily interested in the absorption near and below $E=-0.5$. Therefore, we select x_0 to be that value at which the contributions to $U_2(\rho_2)$ from the Coulomb and linear electric-field potentials are equal when $n_1=n_2=0$, i.e.,

$$x_0^3-2x_0\mathcal{E}^{-1}-\mathcal{E}^{-1}=0. \tag{2.5b}$$

A discussion of the corrections to the model obtained by the use of this value of x_0 is given in Sec. V. The region of space in which the model potential is the Coulomb potential is shown in Fig. 1.

The remaining information needed to specify the model is a statement of our normalization conventions. As the energy spectrum is continuous when $\mathcal{E}\neq 0$, we normalize according to[3,16]

$$\int\bar{\phi}_E(\mathbf{r})\phi_{E'}(\mathbf{r})d^3r=\delta(E-E'). \tag{2.6}$$

The energy delta function arises from the χ_2 contribution to (2.6). In parabolic coordinates, Eq. (2.6) becomes

$$\int_0^\infty d\xi\int_0^\infty d\eta\left[\frac{1}{\xi}+\frac{1}{\eta}\right]\bar{\chi}_{1,E}(\xi)\chi_{1,E'}(\xi)\bar{\chi}_{2,E}(\eta)\chi_{2,E'}(\eta) =\delta(E-E'). \tag{2.7a}$$

Therefore, we can achieve (2.6) by neglecting the less divergent η^{-1} contribution to (2.7a) and adopting the conventions

$$\int_0^\infty \xi^{-1}|\chi_{1,E}(\xi)|^2=1, \tag{2.7b}$$

$$\int_0^\infty \bar{\chi}_{2,E}(\eta)\chi_{2,E'}(\eta)d\eta=\delta(E-E'). \tag{2.7c}$$

We satisfy (2.7b) in our model by straightforward numerical integration. Equation (2.7c) is satisfied by requiring that as $\eta\to\infty$, the probability current density is given asymptotically by $(2\pi\hbar)^{-1}$.

The model potential specified by the above cut-off distance and normalization conventions leads to a Schrödinger equation which can be solved exactly in

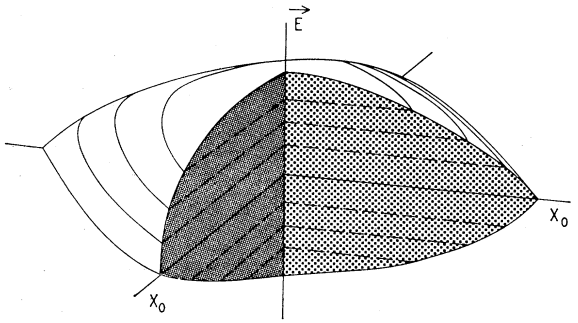

FIG. 1. A cut-away view of the region in which the model potential specified by the cutoff given in Eq. (2.5a) is the Coulomb potential alone.

[16] Reference 15, pp. 16, 60, 71.

terms of the known Kummer[17] and Airy[18] functions. The model is designed to correctly represent those qualitative changes in the wave functions and eigenvalue spectrum wrought by the unbound nature of $\chi_2(\eta)$ at large η. Such a model is essential for even a semiquantitative description of optical absorption in an electric field because a discussion of the low-energy tail on the absorption lies outside the domain of the perturbation theory that describes the Stark shift.[1,4] Furthermore, such a model is required for a description of (exciton) absorption lines associated with hydrogenic levels which are almost auto-ionized by the electric field. The assumptions needed to reduce Eqs. (2.4c) to our solvable model appear less restrictive than those needed to reduce the description of optical absorption in semiconductors to the solution to Eq. (2.1). These latter assumptions include: (a) the validity of the effective-mass approximation,[19] (b) the validity of the Wannier-exciton approximation,[20] and (c) the neglect of electron-phonon coupling. An analog of our model, relevant to the band structure of a particular material, together with its lowest order correction in $(n^3\mathcal{E})$ probably suffices to give as accurate description of optical-absorption experiments as the underlying assumptions warrant.

III. CALCULATION OF THE WAVE FUNCTIONS

For $\rho_i<\rho_i^{(0)}$, the χ_i for our model potential which are finite at the origin are given by[17,21]

$$\chi_i(\rho_i)=c_i n^{1/2}\rho_i^{(1+|m|)/2}\times\exp(-\rho_i/2)M(-n_i,1+|m|,\rho_i);\quad \rho_i<\rho_i^{(0)},\tag{3.1}$$

in which $M(a,b,x)$ is Kummer's function.[17] In the absence of an electric field ($\mathcal{E}=0$), the normalizability of the bound-state wave function requires that the n_i be non-negative integers. For $\rho_1>\rho_1^{(0)}$, the $\chi_1(\rho_1)$ must be a decaying wave function because χ_1 is square-integrable for all energy eigenvalues. The χ_1 model wave function is therefore given by[16,18]

$$\chi_1(\rho_1)=b_1Ai(z_1);\quad \rho_1>\rho_1^{(0)},\tag{3.2a}$$

$$z_1=(n^3\mathcal{E}/4)^{1/3}[(n^3\mathcal{E})^{-1}+\rho_1]\tag{3.2b}$$

in which $Ai(z)$ is the solution to Airy's equation which decays for $z>0$.[18] For $\rho_2>\rho_2^{(0)}$, χ_2 is oscillatory for sufficiently large ρ_2 and is in general a linear combination of two linearly independent solutions to Airy's equation. Taking these to be $Ai(z)$ and $Bi(z)$[18] we get

$$\chi_2(\rho_2)=b_2Ai(z_2)+b_3Bi(z_2);\quad \rho_2>\rho_2^{(0)},\tag{3.3a}$$

$$z_2=(n^3\mathcal{E}/4)^{1/3}[(n^3\mathcal{E})^{-1}-\rho_2].\tag{3.3b}$$

Both the wave functions and their first derivatives must be continuous at $\rho_i=\rho_i^{(0)}$. In the case of χ_1, this boundary condition leads to the quantization of the n_1 quantum number. Continuity of the logarithmic derivative of χ_1 at $\rho_1=\rho_1^{(0)}$ requires that n_1 be a solution to the equation

$$g_{n_1,m}(\rho_1^{(0)})=(\mathcal{E}n^3/4)^{1/3}\frac{Ai'(z_1^{(0)})}{Ai(z_1^{(0)})},\tag{3.4a}$$

$$z_1^{(0)}=(\mathcal{E}n^3/4)^{1/3}[(\mathcal{E}n^3)^{-1}+\rho_1^{(0)}],\tag{3.4b}$$

$$g_{n_1,m}(\rho)=-\tfrac{1}{2}+\frac{1}{\rho}\left\{\frac{1+|m|}{2}+n_i\left[\frac{M(1-n_i,1+|m|,\rho)}{M(-n_i,1+|m|,\rho)}\right]\right\}.\tag{3.5}$$

In the limit that $(n^3\mathcal{E})\to 0$, Eq. (3.4a) becomes

$$\lim_{\rho\to\infty} g_{n_1,m}(\rho)=-\tfrac{1}{2}.\tag{3.6}$$

The use of asymptotic forms of Kummer's function in (3.6) indicates that it is satisfied if n_1 is a non-negative integer. Thus, we recover the results for the Coulomb potential alone in either the zero-field limit ($\mathcal{E}\to 0$) or the large-negative energy ($n\to 0$) limit. In order to achieve these results, it is necessary that $\rho_1^{(0)}\to\infty$ as n or $\mathcal{E}$ goes to zero. If we use a cut-off value of $x_0=\mathcal{E}^{-1/3}$ instead of (2.5b), then the right-hand side of (3.4a) can be expanded as a power series in $\lambda=(n^3\mathcal{E})^{1/3}$. However, this expansion does not appear useful in obtaining an analytical expression for n_1 in the low-λ limit because the Kummer function has an irregular singular point at $\rho_1^{(0)}=\infty$. This property of Kummer functions is closely associated with the computational difficulty that asymptotic forms of $M(a,b,x)$ cannot be used to solve (3.4a). The function $g_{n_1,m}(\rho)$ is a meromorphic function of n_1 for a fixed value of ρ. For small values of $(n^3\mathcal{E})$ its poles and zeros both lie close to the non-negative integers. As $n^3\mathcal{E}$ increases, the poles and zeros become more widely separated, both moving to larger values of n_1. For values of n_1 near its zeros, the Kummer functions in $g_{n_1,m}(\rho)$ cannot be calculated reliably from the large ρ asymptotic form even for $n_1\sim 1$ and $\rho\sim 500$.

The invariant-quantity characteristic of the solutions to (3.4a) is their order. We assign a non-negative integral quantum number $i\geq 0$ to each of the roots of (3.4a) so that $n_1^{(i)}>n_1^{(j)}$ is denoted by $i>j$. In subsequent sections, we present numerical calculations of these roots. The power-series expansion[17] of $M(a,b,x)$ about $x=0$ is used to evaluate the Kummer functions in (3.5) to five significant figure accuracy. The Airy

[17] L. J. Slater, in *Handbook of Mathematical Functions*, edited by M. Abramowitz and I. A. Stegun (U. S. Department of Commerce, National Bureau of Standards, Washington, D. C., 1964), Appl. Math. Ser. **55**, p. 503.
[18] H. A. Antosiewicz, in *Handbook of Mathematical Functions*, edited by M. Abramowitz and I. A. Stegun (U. S. Department of Commerce, National Bureau of Standards, Washington, D. C., 1964), Appl. Math. Ser. **55**, p. 435.
[19] W. Kohn, Solid State Phys. **5**, 258 (1957).
[20] See, e.g., R. S. Knox, Solid State Phys. Suppl. **5**, 1 (1963).
[21] L. D. Landau and E. M. Lifschitz, Ref. 15, p. 130.

functions $Ai(z)$ and $Bi(z)$ are evaluated by a computer program for the GE 235 which employs the methods used by Miller[22] and is accurate to five significant figures.

The continuity of χ_1 at $\rho_1=\rho_1^{(0)}$ is needed to express b_1 in terms of c_1 so that c_1 can be evaluated by the normalization condition (2.7b). The result for c_1 is

$$c_1=n^{-1/2}[I_1+f^2{}_{n_1,m}(\rho_1^{(0)})I_2]^{-1/2}, \tag{3.7a}$$

$$f_{n_i,m}(\rho)=\rho^{(1+|m|)/2} \times\exp(-\rho/2)M(-n_i, 1+|m|, \rho), \tag{3.7b}$$

$$I_1=\int_0^{\rho_1^{(0)}} e^{-x}x^{|m|}M^2(-n_1, 1+|m|, x)dx, \tag{3.7c}$$

$$I_2=\int_{z_1^{(0)}}^{\infty} Ai^2(x)dx/x. \tag{3.7d}$$

The value of c_1 used in subsequent sections is calculated numerically using the trapezoidal rule for I_1 and I_2. I_1 is calculated using 50 intervals of equal length and I_2 is calculated to an accuracy of three decimal places. I_1 is ~ 1 and is usually larger than the second factor in (3.7a) by at least 10^5.

The continuity of χ_2 and its first derivative at $\rho_2=\rho_2^{(0)}$ does not impose any quantization conditions on n_2 and simply gives two relationships which are satisfied by c_2, b_2, and b_3. The value of n_2 to be used in (3.1) is determined for a fixed energy (i.e., value of n) and values of n_1 and m from Eq. (2.4e). A third relation between the (real) values of b_2 and b_3 is obtained from the normalization condition (2.7c), so that all three real constants are determined. We give only the result for c_2

$$c_2=\left(\frac{\pi}{n}\right)^{1/2}\frac{A\cdot Ai(z_2^{(0)})(1-r)}{f_{n_2,m}(\rho_2^{(0)})[r^2+Ai^2(z_2^{(0)})/Bi^2(z_2^{(0)})]^{1/2}}, \tag{3.8a}$$

$$z_2^{(0)}=(n^3\mathcal{E}/4)^{1/3}[(n^3\mathcal{E})^{-1}-\rho_2^{(0)}], \tag{3.8b}$$

$$A=(2\mu)^{1/3}/\pi^{1/2}(|e|F)^{1/6}\hbar^{2/3}, \tag{3.8c}$$

$$r=\frac{g_{n_2,m}(\rho_2^{(0)})+(n^3\mathcal{E}/4)^{1/3}[Bi'(z_2^{(0)})/Bi(z_2^{(0)})]}{g_{n_2,m}(\rho_2^{(0)})+(n^3\mathcal{E}/4)^{1/3}[Ai'(z_2^{(0)})/Ai(z_2^{(0)})]}. \tag{3.8d}$$

If $r=0$, then $b_2=0$ so that inside the $U_2(\rho_2)$ potential barrier the wave function has a purely decaying character. Thus, we identify the value of n at which $r=0$ for a given value of i as determlning the energy $E=-1/2n^2$ at which a quasi-stationary state occurs. A particular value of i contributes a quasi-stationary level near each integral value n_0 of n, $n_0>i$, for values of n_0 up to the point at which autoionization destroys the concept of a quasi-stationary state. Therefore, each root of (3.4a) gives rise to a series of quasi-stationary states in a weak field. More precisely, if $z_2^{(0)}\gtrsim 1$, then a value of $r=0$ causes a sharp peak in c_2. As $\mathcal{E}$ or n increase, the value of $z_2^{(0)}$ decreases until for $z_2^{(0)}\lesssim 1$, the value of c_2 is no longer sensitive to the value of r, and the peaks broaden and disappear. For $z_2^{(0)}>0$, the quantity r exhibits, as a function of n, a dispersion-like behavior characteristic of functions like $\tan(\pi n)$. Its positive and negative asymptotes cause no discernible structure in c_2, although its zeros contribute the quasi-stationary states. For $z_2^{(0)}<0$ and $m=0$, we have never observed a zero in r although single maxima and minima have been seen in numerical computations. This observation indicates, in a well-defined sense, the absence of $m=0$ quasi-stationary states at energies above the top of the $U_2(\rho_2)$ potential barrier.[23]

We finally remark that for small values of $(n^3\mathcal{E})$ an expansion of the expression for r in powers of $(n^3\mathcal{E})^{1/3}$ can be attempted as discussed in conjunction with Eq. (3.4a). In the $(n^3\mathcal{E})\to 0$ limit, we find that to obtain $r=0$ we must require n_2 to be a non-negative integer. Therefore, we recover the results for the Coulomb potential alone.

IV. APPLICATION TO OPTICAL ABSORPTION; NUMERICAL RESULTS

Elliot[12] has shown that the calculation of the absorption coefficient reduces to evaluating the matrix element:

$$M=\sum_{\mathbf{k}_e,\mathbf{k}_h}\Psi_{\mathbf{k}_e,\mathbf{k}_h,j,j'}{}^{\mathbf{K},n}I_{jj'}(\mathbf{k}_e,\mathbf{k}_h,\xi,\mathbf{q}), \tag{4.1a}$$

$$I_{jj'}(\mathbf{k}_e,\mathbf{k}_h,\xi,\mathbf{q}) =\int d^3r\psi_{\mathbf{k}_e,j}{}^{+}(\mathbf{r})e^{i\mathbf{q}\cdot\mathbf{r}}\frac{ieh}{m}\xi\cdot\nabla\psi_{\mathbf{k}_h,j'}(\mathbf{r}), \tag{4.1b}$$

in which $\mathbf{q}$ is the wave vector and ξ the polarization vector of the optical field; $\mathbf{k}_e$ and $\mathbf{k}_h$ are the wave vectors of the electron and hole from bands j and j' respectively; the $\psi_{\mathbf{k},j}$ are their one-electron wave functions, and the Ψ are the Fourier transforms of exciton wave functions with center-of-mass momentum $\mathbf{K}$ and relative quantum number n. The exciton is composed of the electron and hole whose motion for $\mathbf{K}=0$ is described by equation (2.1) in which we make the identifications (for $\hbar\omega<E_g$),

$$\mu=m_jm_{j'}/(m_j+m_{j'}), \tag{4.2a}$$

$$E=(\hbar\omega-E_g)/E_0\equiv -1/2n_\omega^2, \tag{4.2b}$$

[22] J. C. P. Miller, *The Airy Integral* (Cambridge University Press, Cambridge, England, 1946). Copies of the FORTRAN program are available as General Electric Research and Development Center Report No. 65-C-045 (unpublished).

[23] Although this remark is by no means "proof" of the absence of such states, it should be contrasted with the semiclassical results for $m>1$ as presented, for example, in Fig. 3 of Ref. 1(a). See also H. A. Bethe and E. E. Salpeter, *Quantum Mechanics of One- and Two-Electron Atoms* (Academic Press Inc., New York, 1957), p. 238.

with m_j denoting the effective mass in the jth band, $\hbar\omega$ being the energy of the absorbed photon, and E_g signifying the zero-field band gap. The electric field makes two modifications in M from the field-free case. First, the expansion coefficients, Ψ, are changed because their Fourier transform satisfies (2.1) in lieu of the Schrödinger equation with the Coulomb potential alone. Second, the matrix elements $I_{jj'}$ are also altered because the one-electron wave functions $\psi_{\mathbf{k}_e,j}$ are modified by the intra-cell components of the electric field. We treat both the external electric field and the Wannier-exciton correlations in the effective-mass approximation in which the second modification is neglected. We could improve the effective-mass approximation by using the intra-cell components of the field to define a modified band structure,[24] but the corrections so introduced are thought to be negligible for nondegenerate bands.[25] Furthermore, the integrals $I_{jj'}$ in (4.1b) are usually treated as phenomenological parameters used to fit experimental data.[26] Therefore, we directly utilize Elliot's results and terminology.[12] A study of the modification of the selection rules imposed by the symmetry of particular crystals[25,27] is not undertaken.

For vertical transitions (called "allowed" transitions by Hopfield[27]), it is well known that the absorption coefficient α is given by[10,12]

$$\alpha(\omega)=\frac{4\pi^2e^2}{n'cm^2\omega}\sum_f|P_{if}|^2\delta(E_g+E_f-E_i-\hbar\omega), \tag{4.3a}$$

$$P_{if}=\phi_{Ef}(0)C_0a_B^{-2}\ \text{(allowed transitions)}, \tag{4.3b}$$

$$P_{if}=(\nabla_\xi\phi_{Ef})(0)\cdot C_1a_B^{-2}\ \text{(forbidden transitions)}. \tag{4.3c}$$

The subscript i denotes the initial state of the crystal which we take to be the filled valence and empty conduction bands and to have $E_i=0$. The dipole matrix element of the transition is given by P_{if} in which f denotes the internal quantum numbers of the final exciton state. The quantities n' and c are the high-frequency index of refraction and the speed of light respectively. The a_B^{-2} in (4.3a) and (4.3b) results from our use of atomic units in (2.1). The C_0 and C_1 are constants which are simply related to the $I_{jj'}(\mathbf{k}_e,\mathbf{k}_h,\mathbf{q}=0,\xi)$ in (4.1b) in the cases that it does and does not vanish at $\mathbf{k}_e=\mathbf{k}_h=0$.[12] The quantum numbers f are the index i of $n_1^{(i)}$ and the dimensionless energy variable E. It is convenient to define

$$|G(n,n_1^{(i)})|^2=|c_1(n,n_1^{(i)})|^2|c_2(n,n_1^{(i)})|^2/\pi A^2Ai^2(z_2^{(0)}) \tag{4.4}$$

in terms of (3.7) and (3.8) such that G is dimensionless and depends only on ratios of Airy functions. The absorption coefficient for allowed transitions can be written in the form

$$\alpha(\omega)=(P/\omega)\sum_{i=0}^{\infty}\alpha_i(\mathcal{E},\omega), \tag{4.5a}$$

$$\alpha_i(\mathcal{E},\omega)=\mathcal{E}^{-1/3}|\phi_{i,n_\omega,\mathcal{E}}(0)|^2, \tag{4.5b}$$

$$|\phi_{i,n,\mathcal{E}}(0)|^2=Ai^2(z_2^{(0)})|G(n,n_1^{(i)})|^2, \tag{4.5c}$$

$$P=2^{11/3}\pi e^2C_0^2/n'cm^2E_0a_B^3, \tag{4.5d}$$

in which $z_2^{(0)}$ is defined by Eq. (3.8b) and n_ω by Eq. (4.2b). We refer to $|\phi_{i,n,\mathcal{E}}(0)|^2$ as the strength function for an allowed transition. All of the properties of the specific material are incorporated in the scale factor P and the quantities a_B and E_0. The α_i are the contributions to the optical absorption associated with the ith root of (3.4a). They have been written in a manner to suggest the decomposition into the free-particle-like factor $\mathcal{E}^{-1/3}Ai^2(z_2^{(0)})$ and a "Sommerfeld" factor $|G|^2$. We noted in Sec. II that each value of i gives rise to a series of absorption peaks near integral values, n_0, of n_ω for $n_0>i$ below the auto-ionization limit. The utility of the series in (4.5a) results from the fact that for n_ω near its lower integral values, only a few terms of the series need to be considered. Therefore, our model provides a practical method of computing the absorption coefficient in the region of the lower exciton peaks below the free-electron band edge.

The requirement that the appropriate dipole matrix element in (4.3) be nonvanishing provides selection rules for the values of m associated with allowed and forbidden transitions. It is easily verified from the indicial equation associated with Eqs. (2.4) that $m=0$ if $\phi_E(0)$ is to be nonvanishing.[28] Therefore, each of the zero-field exciton lines at $n=n_0$ splits up into n_0 components under the influence of an electric field. In the case of forbidden transitions, the selection of $m=0$ leads to absorption lines for optical polarizations parallel to the external field.[28] Furthermore, for $n_0=2k+1$, we find a line for which $n_1=n_2=k$ that does not occur for $\mathcal{E}=0$ but does occur when $\mathcal{E}\neq0$. There are not enough of these lines to account for the "weak" lines in Cu_2O,[25,29] so that the originally proposed[29] breakdown of the l degeneracy in the simple hydrogenic model must be considered as the cause of some of these weak lines. The absorption via forbidden transitions of light polarized perpendicular to $\mathbf{F}$ is associated with $m=\pm1$.[28] The selection rules for forbidden transitions correspond to those for atomic transitions in the strong-field Stark effect.[1]

Numerical calculations based on the strong-field model of Sec. II predict that a strong electric field causes three qualitative alterations of the Stark spectra: the Stark lines broaden appreciably, rapidly lose their

[24] See, E. I. Blount, Solid State Phys. **13**, 306 (1962).
[25] H. Haken, *Proceedings of the International Conference on the Physics of Semiconductors, Exeter, 1962* (Institute of Physics and the Physical Society, London, 1962), p. 462; J. B. Grun and S. Nikitine, J. Phys. Radium **23**, 159 (1962).
[26] B. O. Seraphin and N. Bottka, Phys. Rev. **139**, A560 (1965).
[27] J. J. Hopfield, J. Phys. Chem. Solids **15**, 97 (1960).
[28] This result is independent of the use of a model potential.
[29] E. F. Gross, Nuovo Cimento Suppl. **3**, 672 (1965) and references contained therein.

intensity, and finally meld into a downward moving "continuum edge" at energies above which an exciton is ionized by the electric field. All three effects are evident in Fig. 2. The $n_0=2$ peaks at $(E_g-\hbar\omega)/E_0\cong 0.125$ have already vanished at $\mathcal{E}=0.05$ and hence are not visible in the figure. The motion of the continuum edge is particularly evident in the raising of the value of the strength function in the region between the $n_0=1$ and $n_0=2$ zero-field peaks. A more detailed study of the $n_0=1$ line is given in Fig. 3. The qualitative aspects of the absorption constant shown in Figs. 2 and 3 have been considered by several authors[3,4,11,25,29,30] among whom Gross[29] gave the first comprehensive discussion of the application to exciton absorption. However, Figs. 2 and 3 represent the first quantitative calculations giving values for the absorption coefficient which show the details of the line shape and the movement of the continuum edge. The agreement between the features predicted by the above calculations for allowed transitions and the features observed by Gross for forbidden transitions[31] is strong supporting evidence for his interpretation of the Cu_2O data. In Fig. 4 we show the two $n_0=2$ lines at $\mathcal{E}=0.01$, just before they disappear into the continuum edge. The fact that the higher energy line is narrower than its low-energy counterpart

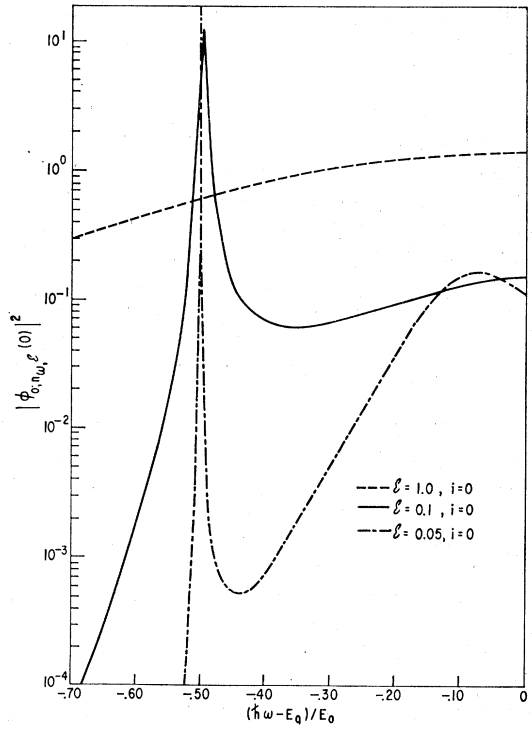

FIG. 2. Strength functions associated with allowed transitions at energies $E=-(E_g-\hbar\omega)/E_0$ near the first ($E=-0.5$) and second ($E=-0.125$) exciton peaks. The calculations were performed using only the $i=0$ term in Eqs. (4.5), (4.4), (3.8), and (3.7) of the text.

[30] J. J. Hopfield and D. G. Thomas, Phys. Rev. **122**, 35 (1961).
[31] See especially Fig. 13 in Ref. 29.

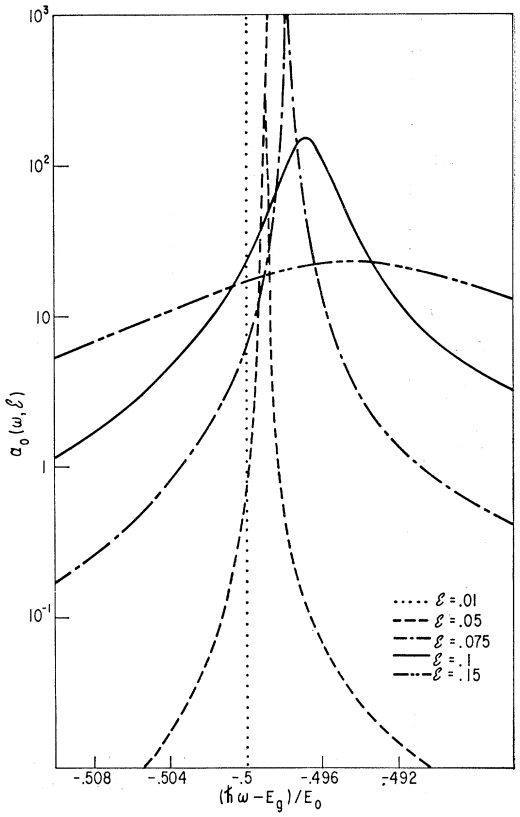

FIG. 3. The reduced absorption coefficient for allowed transitions in the vicinity of the first exciton peak. The calculations were performed using only the $i=0$ term in Eqs. (4.5), (4.4), (3.8), and (3.7) in the text.

is reminiscent of the behavior of the $n=3$, $n''-3$, and $n'''-3$ lines in Cu_2O.[29] The origin of this behavior is identical with that of the red $H\gamma$ Balmer line fading prior to the violet $H\gamma$ line in an increasing external field.[4] The higher energy $i=1$ state has a larger probability of being on the side of the Coulomb potential through which no leakage takes place (the "ξ" side) whereas the $i=0$ state has a larger probability of being on the side with the leaky barrier (the "η" side).

Figures 2 and 3 need not represent numerically accurate model predictions because they are calculated using only the first term of the sum in (4.5a). The values of the strength function associated with the second term are shown in Fig. 5. It is only for $(\hbar\omega-E_g)/E_0>-0.08$ that the $i=1$ term comes within an order of magnitude of the $i=0$ term. The $i=2$ term is reduced further by a factor ~ 100. Therefore, Figs. 2 and 3 represent quantitative predictions of the absorption coefficient based on the model potential. The corrections to Fig. 4 due to the $i=2$ term are small. The model potential tends to overestimate the stability of the exciton peaks relative to the exact Coulomb potential. Therefore within the framework of the Elliot model of optical absorption, from Figs. 2, 3, and 4 we conclude that $\mathcal{E}=0.15$ is an upper bound on the field at which any exciton peaks

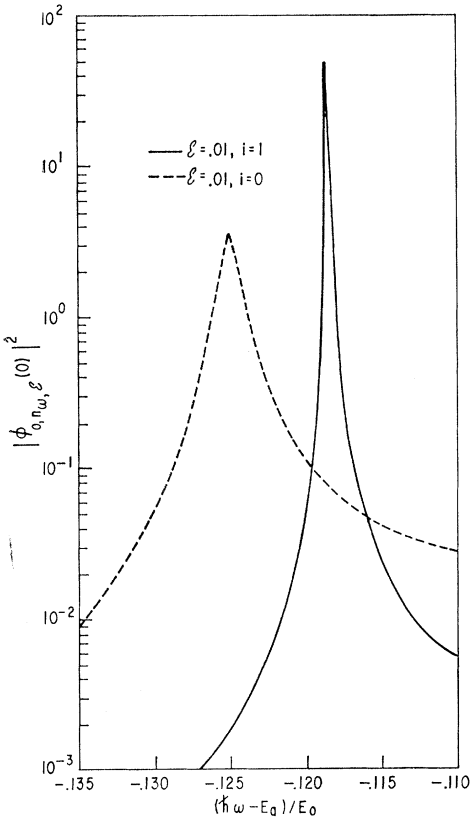

FIG. 4. Strength functions associated with allowed transitions at energies $E=-(E_g-\hbar\omega)/E_0$ near the second ($E=-0.125$) exciton peak. The calculations were performed using the $i=0$ and $i=1$ terms in Eqs. (4.5), (4.4), (3.8), and (3.7) in the text.

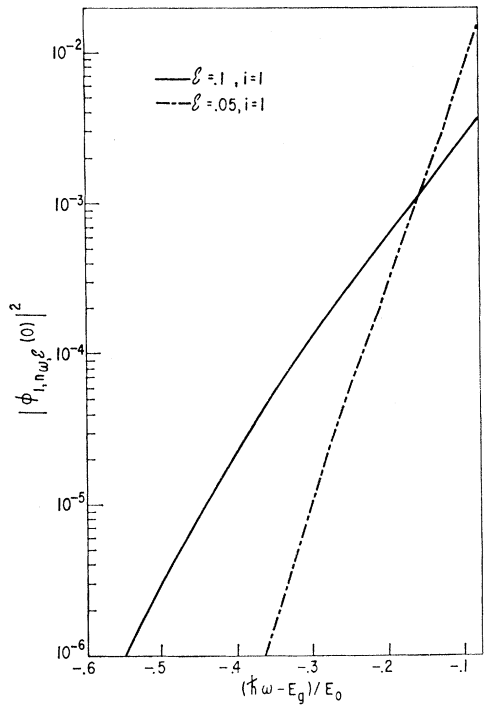

FIG. 5. Strength functions associated with allowed transitions at energies $E=-(E_g-\hbar\omega)/E_0$ near the first ($E=-0.5$) and second ($E=-0.125$) exciton peaks. The calculations were performed using only the $i=1$ term in Eqs. (4.5), (4.4), (3.8), and (3.7) in the text.

occur and $\mathcal{E}=0.05$ is an upper bound on the field at which $n_0=2$ peaks occur.

An application of these results occurs in the identification of structure in electric-field-modulated absorption or reflectivity data due to excitons. There are no published absorption measurements in direct-band-gap semiconductors to which the lineshapes of Figs. 2, 3, and 4 directly apply.[31a] We have already discussed the Cu_2O experiments.[25,29] The experiments of Moss[32] on GaAs were performed at too high temperatures to see exciton structure. Lambert[33] has extended the measurements down to temperatures of 85°K for fields above 5.38×10^3 V/cm. The $\mathcal{E}=0.15$ upper bound yields a field of 1.7×10^3 V/cm above which exciton peaks associated with the direct band gap at the center of the Brillouin zone should not be observed in GaAs. Lambert's data is consistent with this prediction. Furthermore, at the lower values of the electric field which he considered ($F=1.076\times10^4$ and 5.38×10^3 V/cm), his data exhibits a much sharper edge than the Franz-Keldysh Theory predicts. We identify this edge (which lies below the zero-field edge) with the continuum edge which has been lowered by the electron-hole Coulomb interaction. At the larger values of the field, the sharp edge is smeared out into the more gradual Franz-Keldysh result because the tunneling probability becomes quite large at all energies near the band gap. The experiments of Hopfield and Thomas on CdS[30] were performed at too low fields ($\mathcal{E}\lesssim5\times10^{-3}$) and in CdS the hydrogenic model of the exciton states must be modified because of crystal-symmetry effects and spin-orbit mixing of the valence bands.

The application of Figs. 2–4 to determine the lineshapes of electric-field-modulated reflectance data is rather tentative because one must know the reflectivity data at all frequencies to obtain the absorption coefficient. In regions where extensive structure occurs in the reflectivity, the direct inference of the structure in $\alpha(\omega)$ from the reflectivity data is unwarranted. However, we can apply our upper limits on the fields strengths to determine when excitonic structure in the reflectivity is possible. Thus, for example, using Seraphin and Bottka's[26] parameters for the indirect edge in Ge, we expect no $n_0=1$ exciton structure for fields above $F=900$ V/cm. In *Si*, using the estimates of the parabolic exciton binding energy of 7 MeV$<E_B<$14 MeV given by Phillips and Seraphin[34] we predict that the

[31a] See *Note added in proof.*
[32] T. S. Moss, J. Appl. Phys. Suppl. **32**, 2136 (1961).
[33] L. M. Lambert, J. Phys. Chem. Solids **26**, 1409 (1965).
[34] J. C. Phillips and B. O. Seraphin, Phys. Rev. Letters **15**, 107 (1965).

structure due to the direct exciton cannot be seen above $2.5\times10^3<F<10^4$ V/cm.[35] The larger mass of the exciton along the $\Gamma-X$ line in *Si* renders it observable to $F=7\times10^4$ V/cm, thus tenatively confirming the interpretation of the indirect absorption data given by Wendland.[8,36]

A final prediction of the model is that asymptotically for photon energies such that $n^3\mathcal{E}\ll1$, the Franz-Keldysh[10] dependence of the absorption coefficient on $\exp(-2/3n^3\mathcal{E})$ is unchanged by the Coulomb potential. The sum over i in Eqs. (4.5) cannot be performed analytically even in this limit, but by using integral values of $n_1^{(i)}$, we can estimate the sum and show that corrections to the exponent in α are small. As $n\to0$ for a fixed value of $\mathcal{E}$ one finds $c_1\to n^{-1/2}$. There are no Stark levels in the asymptotic tail so that r defined by (3.8d) is nonzero. (The precise value of r depends on the value of n_1 for a fixed value of n.) Hence, by use of the asymptotic forms for Airy functions,[18] we find that for allowed transitions ($m=0$)

$$|G(n,n_1^{(i)})|^2=1/n^2f^2{}_{n_1-n+1,m=0}(\rho_2^{(0)}). \qquad (4.6)$$

For $|n_1|<[\rho_2^{(0)}]^3$, Eq. (13.5.1) in Ref. 17 shows that $|G|^2\sim\exp(\rho_2^{(0)})$. For $|n_1|>[\rho_2^{(0)}]^3$, the sum in (4.5a) is replaced by an integral and Eq. (13.5.13) in Ref. 17 is used for the Kummer function to show that the sum is $\sim\exp[-(\rho_2^{(0)})^2]$. Both of these contributions from the $|G|^2$ yield additive contributions to the exponent in the absorption coefficient whose leading term is the Franz-Keldysh factor $\exp(-2/3n^3\mathcal{E})$ contributed by the $Ai^2(z_2^{(0)})$ in Eq. (4.5c). Hence, in the limit that $n^3\mathcal{E}\ll1$, the Sommerfeld-like factor $|G|^2$ contributes an amount to the exponent negligible relative to the Franz-Keldysh leading term, for all x_0 such that $[\rho_2^{(0)}]^2\ll(n^3\mathcal{E})^{-1}$. Equations (2.5) prescribe such a value of x_0.

V. DISCUSSION

To discuss the accuracy with which the model potential approximates the actual potential, we consider separately two energy regions. The extension of the Coulomb wave function of energy $-1/2n^2$ is $\sim n$ (in atomic units) so that the maximum potential energy gained by a particle-hole pair in this state is $\Delta E\sim n\mathcal{E}$. For perturbation theory to be a valid treatment of the electric field, $1/2n^2\ll\mathcal{E}n$ or $n^3\mathcal{E}\ll\frac{1}{2}$. Therefore, we decompose the negative-energy spectrum on the basis of the parameter $n^3\mathcal{E}$.

Region I: $n^3\mathcal{E}\lesssim1$

In this region, perturbation theory is approximately valid. The well-known expression[1] for the Stark-shift energy is an asymptotic expansion in $(n^3\mathcal{E})$ which diverges after the first term for $n^3\mathcal{E}\geq0.036$. (The equality sign applies for $n=1$.) The cutoff specified by Eqs. (2.5) gives $x_0>n$ so that the model eliminates the electric field in the region where the Coulombic wave function is large. Therefore, the model constitutes an almost equivalent starting point to the Coulomb potential alone for the calculation of Stark shifts. (For example, the energy shifts in Fig. 3 are always at least a factor of five smaller in magnitude than the quadratic Stark shift.) Although it misplaces the level positions, the model should more accurately predict their widths and the intra-level absorption because it correctly describes the free-electron-like states for large values of η which cause the latter phenomena. However, in this region the model appears to be considerably less accurate than the quasiclassical approximation to the solution of the exact Schrödinger equation developed by Lanczos[4] for $m>1$.

Region II: $n^3\mathcal{E}\gtrsim1$

Perturbation theory is invalid in this region. If $m>1$, quasiclassical motions can be investigated by use of the WKBJ approximation.[1,4,15] For the values of $m=0$, 1 of interest in the optical absorption problem, the model constitutes the only currently available technique for discussing the eigenfunctions in this region of energies. However, away from the origin the WKBJ phase-integral methods can be applied to determine approximate solutions to Eq. (2.4c).

The major difficulty with the model potential lies in the fact that we have not established the sensibility of a state-independent cutoff distance. For values of n_1 which are small, Eq. (2.5b) gives a sensible approximate potential. However, when n_1 is large, the U_2 model potential can be noticably altered in shape from the exact potential. This difficulty is not severe for the calculations presented in the figures for which $n_1\lesssim1$. Therefore, we anticipate that our numerical lineshapes would not be greatly changed by a more accurate calculation.

A second difficulty, not directly related to our use of a model potential, occurs because near $E=0$ all of the terms in the sum of Eq. (4.5a) become large so that approximations become inaccurate. This factor appears to be the limiting one of either a model such as we propose, or any more accurate calculation in which the sum is not performed analytically.

Despite the above difficulties, the model does provide an upper bound for the value of the electric field at which an absorption peak due to a low-energy parabolic Wannier exciton is quenched. This quantitative information is useful in discussing the spatial extent of an exciton state which gives rise to a peak in the absorption

---

[35] Although Seraphin and Bottka (Ref. 9) do not give the peak value of the electric field used in their measurements on Si, the value used by Seraphin and Hess is 10^5 V/cm. Therefore, the parabolic exciton is probably ionized by the field and causes no structure in the reflectance data independent of the resolution difficulties discussed in Ref. 34.

[36] Wendland's estimate of the auto-ionization energy for the $n_0=1$ exciton peak should have been made using the quadratic rather than the linear Stark shift.

coefficient. The low values of the quenching fields obtained in the last section (e.g., for the direct exciton in GaAs reflect both the small conduction-band masses and the large static dielectric function. In the alkali halides, the effective masses are ~ 1, but the factor of ϵ_0^3 in (2.1b) can reduce the quenching field by a factor $\sim 10^2-10^3$. However, such a reduction only occurs for large excitons. As the extent of the exciton diminishes, the various many-body processes which give rise to the occurence of ϵ_0^3 in (2.1b) are no longer effective.[37] Hence, "small" excitons are associated with peaks which quench at fields larger than that predicted using ~ 0.15 in (2.1b). Thus, the fields at which the two lowest exciton peaks in the alkali halides quench can distinguish whether they are adequately described by the Wannier model[38,39] or perhaps are more molecular in nature. Similar considerations also apply to the hypothesis of "saddle-point" excitons in the alkali halides and rare-gas solids.[38] In particular, the measurement of the sensitivity of exciton peaks to an electric field affords a more convenient and equally reliable method of determining the spatial extent of excitons than melting the crystal.[40]

Summarizing, we propose a model of a hydrogenic system in a strong electric field which explicitly incorporates the unbound character of the wave functions, but for which the Schrödinger equation can be solved analytically in terms of known functions. Following Elliot's[12] formalism, we derive formulas for the absorption coefficient in an external field in terms of the wave functions of a hydrogenic system in that field. The relevant selection rules are obtained and for allowed transitions the model wave functions are utilized to calculate the absorption coefficient for photon energies just below the direct band-gap energy. For photon energies far below the band-gap, we show that the model predicts that the Franz-Keldysh "free-electron" exponential absorption is essentially unchanged by the Coulomb electron-hole interaction. The numerical model predictions for the optical absorption are shown to be consistent with experiments in GaAs, Cu_2O, Si, and Ge. However, the model should be most applicable to a discussion of the optical absorption in a direct semiconductor with cubic symmetry like GaAs or cubic ZnS. In such a material, the disappearance of the lowest two exciton peaks and lowering of the continuum absorption edge should be semiquantitatively predicted by the model, and is observable in samples in which the intrinsic exciton line-width is small enough to observe the zero-field window between these exciton absorption peaks.

Note added in proof. Since the submission of this manuscript, Dr. Q. H. F. Vrehen[41] has measured the dependence of the direct exciton peak in Ge on the electric field strength. He finds that the peak disappears near $F=933$ V/cm and that its width is linear in F. Our model predicts that the light-hole peak ($\mu=0.021m$) disappears at 85 V/cm and the heavy hole peak ($\mu=0.036m$) disappears at 250 V/cm. The failure of our model to describe the line shape is due to our neglect of mechanisms which cause the large intrinsic width of the exciton peak in Ge. The only qualitative success of the model in predicting the peak's disappearance could be caused by either the above shortcoming of the model or by the inadequacies of the parabolic-band effective mass approximation.

ACKNOWLEDGMENTS

The authors are indebted to Dr. G. D. Mahan for stimulating conversations, the staff of the computer unit at the General Electric Research and Development Center for making available extra computing time on short notice, and to Dr. Q. H. F. Vrehen for communication of his results prior to publication.

[37] See, H. Haken, *Polarons and Excitons*, edited by C. G. Kuper and G. D. Whitfield (Plenum Press, Inc., New York, 1963), p. 295.
[38] J. C. Phillips, Phys. Rev. 136, A1705 (1964).
[39] J. J. Hopfield and J. M. Worlock, Phys. Rev. 137, A1455 (1965).
[40] D. Beaglehole, Phys. Rev. Letters 15, 551 (1965).
[41] Q. H. F. Vrehen, Phys. Rev. 145, 675 (1966).